

# Synthesis of magnetically recyclable $\text{Fe}_3\text{O}_4@[(\text{EtO})_3\text{Si}-\text{L}^1\text{H}]/\text{Pd}(\text{II})$ nanocatalyst and application in Suzuki and Heck coupling reactions

Hassan Keypour<sup>a\*</sup>, Shokoufeh Ghahri Saremi<sup>a</sup>, Mohammad Noroozi<sup>b</sup> and Hojat Veisi<sup>c</sup>

A Pd(II) Schiff base complex as an efficient and highly heterogeneous catalyst was developed by immobilization of a palladium complex on the surface of modified  $\text{Fe}_3\text{O}_4$  magnetite nanoparticles. These surface-modified nanoparticles were characterized using various techniques such as transmission electron microscopy, X-ray diffraction, thermogravimetric analysis, vibrating sample magnetometry, elemental analysis and Fourier transform infrared spectroscopy. The palladium catalyst exhibited efficient catalytic activity in Suzuki and Heck coupling reactions. This method has notable advantages such as excellent chemoselectivity, mild reaction conditions, short reaction times and excellent yields. The yields of the products were in the range 85–100%. Also, the nanocatalyst can be easily recovered with a permanent magnet and reused at least five times without noticeable leaching or loss of its catalytic activity. Copyright © 2016 John Wiley & Sons, Ltd.

**Keywords:** schiff base complex;  $\text{Fe}_3\text{O}_4$  nanoparticles; palladium; suzuki; coupling reactions

## Introduction

Over the last few years significant progress has been made in the development of new inorganic catalytic systems which are immobilized onto magnetic nanocarriers. Normally, to protect a magnetic core and retain magnetic properties, the core is coated with some non-magnetic relatively inert shell such as silica. The silica shell is very easy to functionalize and good for binding of various catalytic species including transition metal complexes.<sup>[1–6]</sup> Additionally, the magnetic properties make the recovery of the catalyst possible by means of an external magnetic field. These advantages are even more attractive if such reactions can be conducted in aqueous media.<sup>[7–14]</sup>

The Suzuki cross-coupling reaction is an important method for the selective construction of biaryls,<sup>[15]</sup> and has found extensive use in the synthesis of natural products, pharmaceuticals and advanced materials.<sup>[16]</sup> The utility of the Suzuki reaction derives from its high stability, broad functional group tolerance and the low toxicity associated with boron compounds. Recently, the use of water as solvent for the Suzuki reaction has received much attention.<sup>[17]</sup>

Palladium-catalysed Suzuki reactions between aryl halides and phenylboronic acid continue to attract attention because of their versatility and the potential of the products formed. The area that has perhaps received most research is the development of new catalysts and ligands for Suzuki coupling reactions, and the use of these catalyst systems in, for example, natural product synthesis.<sup>[18]</sup> In the past few years, attempts have been devoted to the development of new soluble palladium complexes as highly active catalysts for this reaction.<sup>[19,20]</sup>

Homogeneous catalysis is generally connected with the problem of separation and wasted inorganics which are too difficult to reuse. In addition, deactivation of soluble palladium complex catalysts by formation of inactive metal particles is often encountered at high reaction temperature. These problems could be principally minimized by a heterogeneously catalysed Suzuki reaction.<sup>[21]</sup>

Schiff base transition metal complexes have been extensively studied because of their potential use as catalysts in a wide range of reactions.<sup>[22,23]</sup> These complexes have been extensively used for hydrogenation of organic substrates,<sup>[24]</sup> epoxidation of olefins,<sup>[25]</sup> conversion of epoxides into halohydrins,<sup>[26,27]</sup> asymmetric ring opening of terminal epoxides<sup>[28]</sup> and oxidation reactions.<sup>[29,30]</sup> Therefore, here we report the further chemical modification of surface-tethered amino groups with Schiff base ligands through reaction between amine and aldehyde groups of 4-hydroxy-3-methoxybenzaldehyde to form corresponding imines. Also, we studied the catalytic behaviour of a Pd(II) complex of the tethered Schiff base ligand as a heterogeneous catalyst in the cross-coupling reaction between aryl halides and phenylboronic acid.

\* Correspondence to: Hassan Keypour, Faculty of Chemistry, Bu-Ali Sina University, Hamedan 65174, Iran. E-mail: haskey1@yahoo.com

a Faculty of Chemistry, Bu-Ali Sina University, Hamedan 65174, Iran

b Center for Research and Development of Petroleum Technologies at Kermanshah, Research Institute of Petroleum Industry (RIPI), Iran

c Department of Chemistry, Payame Noor University, Tehran, Iran

## Experimental

### Materials and Instrumentation

The reagents and solvents used in this work were obtained from Fluka or Merck and used without further purification. Nanostructures were characterized using a Holland Philips PW-1840 with monochromated Cu K $\alpha$  radiation and  $\lambda$  1.54 Å X-ray powder diffraction (XRD) diffractometer, at a scanning speed of 2°/min from 5° to 80°(2 $\theta$ ). Magnetic measurement of materials was investigated with a vibrating sample magnetometer (VSM) at room temperature. The particle size and morphology shape were investigated by scanning electron microscopy (SEM) of a Holland Philips XL30 microscope with an accelerating voltage of 25 kV. The FT-IR measurements were performed using KBr disc on a Shimadzu Fourier Transform Infrared spectra (FT-IR) 8400. The <sup>1</sup>H- and <sup>13</sup>C-spectra were measured at 90 MHz, on a Bruker DRX 500-Avance FTNMR instrument with CDCl<sub>3</sub> as the solvent. Elemental analysis for C, H and N were performed using a Perkin-Elmer 2400 series analyzer. Thermogravimetric Analysis (TGA) was taken on a Mettler Toledo TGA SDTA 85-e instrument at 30-800°C with 10 °C/Min. Transmission electron microscopy (TEM) images were obtained on an EM10C (Zeiss) transmission electron microscope at an accelerating voltage of 80 kV.

### Preparation of Fe<sub>3</sub>O<sub>4</sub> Magnetic Nanoparticles (MNPs)

Fe<sub>3</sub>O<sub>4</sub> MNPs were prepared by the conventional co-precipitation method.<sup>[31]</sup> Firstly, 4.6704 g (17.28 mmol) of FeCl<sub>3</sub>·6H<sub>2</sub>O and 1.7176 g (8.64 mmol) of FeCl<sub>2</sub>·4H<sub>2</sub>O were dissolved in 100 ml of deionized water at 85 °C under nitrogen atmosphere and with vigorous mechanical stirring (500 rpm). Aqueous ammonia solution (10 mL, 25%) was then quickly added into the solution with vigorous stirring, followed by more ammonia solution until the formation of a black precipitate of MNPs, and then the solution was stirred for an additional 30 min. The mixture was finally cooled to room temperature, the precipitates were collected using a magnet and washed several times with deionized water and twice with ethanol.

### Preparation of *N*-(Triethoxysilylpropyl)salicylaldehyde Schiff Base Ligand ((EtO)<sub>3</sub>Si-L<sup>1</sup>H)

The Schiff base organosilane ligand was synthesized according to a reported procedure.<sup>[32]</sup> A solution of (3-aminopropyl) triethoxysilane (APTES; 2.21 g, 10.0 mmol) in methanol (10 ml) was added to a solution of 4-hydroxy-3-methoxybenzaldehyde (1.52 g, 10.0 mmol) in methanol (10 ml). The colourless solution immediately turned yellow. The reaction was maintained under reflux for 2 h and then the solvent was removed by rotary evaporation under reduced pressure. The resulting viscous yellow oil was dissolved in dichloromethane and washed repeatedly with water. The organic layer was separated and dried over anhydrous magnesium sulfate followed by solvent evaporation and drying at room temperature for several hours. Yield 2.30 g, 71.0%. FT-IR (KBr, cm<sup>-1</sup>): 3449 (O-H), 3065, 2977, 2930, 2894, 2744, 1661 (C=N, imine), 1585 (m).

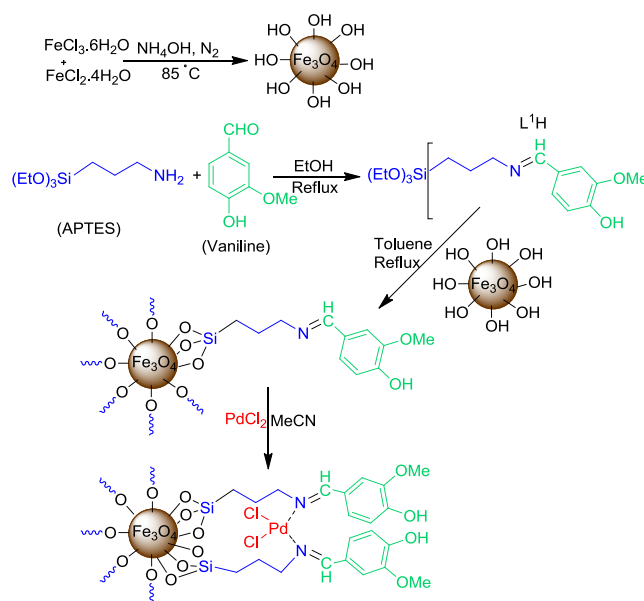
### Preparation of Fe<sub>3</sub>O<sub>4</sub>@[(EtO)<sub>3</sub>Si-L<sup>1</sup>H]

The (EtO)<sub>3</sub>Si-L<sup>1</sup>H Schiff base ligand was anchored onto Fe<sub>3</sub>O<sub>4</sub> MNP surface via a grafting method. A 1.0 g sample of pretreated Fe<sub>3</sub>O<sub>4</sub> powder was suspended in 50 ml of dry toluene in a round-

bottomed flask (100 ml) which was flushed with nitrogen. (EtO)<sub>3</sub>Si-L<sup>1</sup>H (3.99 g) was then added and the suspension stirred for 24 h under reflux in nitrogen atmosphere. The resulting suspension was filtered and washed with Et<sub>2</sub>O (3 × 15 ml). The recovered powder was extracted in a Soxhlet apparatus using refluxing CH<sub>3</sub>OH (750 ml) for 24 h. The functionalized Fe<sub>3</sub>O<sub>4</sub>, designated as Fe<sub>3</sub>O<sub>4</sub>@[(EtO)<sub>3</sub>Si-L<sup>1</sup>H], was dried under vacuum at room temperature for 18 h. A brown powder was recovered. FT-IR (KBr, cm<sup>-1</sup>): 3444 (m, br), 2930 (w), 2864 (w), 1661, 1084, 806, 466.

### Preparation of Fe<sub>3</sub>O<sub>4</sub>@[(EtO)<sub>3</sub>Si-L<sup>1</sup>H]/Pd(II)

Fe<sub>3</sub>O<sub>4</sub>@[(EtO)<sub>3</sub>Si-L<sup>1</sup>H] (300 mg) was dispersed in CH<sub>3</sub>CN (30 ml) using an ultrasonic bath for 30 min. Subsequently, a yellow solution of PdCl<sub>2</sub> (25 mg) in 30 ml of acetonitrile was added to the dispersion of Fe<sub>3</sub>O<sub>4</sub>@[(EtO)<sub>3</sub>Si-L<sup>1</sup>H] and the mixture was stirred for 10 h at room temperature. Then, Fe<sub>3</sub>O<sub>4</sub>@[(EtO)<sub>3</sub>Si-L<sup>1</sup>H]/Pd(II) was separated by magnetic decantation and washed successively with CH<sub>3</sub>CN, water and acetone to remove the unattached substrates (Scheme 1). The palladium content in the Fe<sub>3</sub>O<sub>4</sub>@[(EtO)<sub>3</sub>Si-L<sup>1</sup>H]/Pd(II) catalyst was determined as 4.31 wt.% using atomic absorption spectroscopic analysis. The prepared catalyst was characterized using FT-IR spectroscopy, XRD, SEM, energy-dispersive X-ray spectroscopy (EDX), transmission electron microscopy (TEM), inductively coupled plasma (ICP) analysis and vibrating sample magnetometry. The reduction of Fe<sub>3</sub>O<sub>4</sub>@[(EtO)<sub>3</sub>Si-L<sup>1</sup>H]/Pd(II) using hydrazine hydrate was performed as follows: 50 mg of Fe<sub>3</sub>O<sub>4</sub>@[(EtO)<sub>3</sub>Si-L<sup>1</sup>H]/Pd(II) was dispersed in 60 ml of water, and then 100 μl of hydrazine hydrate (80%) was added. The pH of the mixture was adjusted to 10 with 25% ammonium hydroxide and the reaction was carried out at 95 °C for 2 h. The final product, Fe<sub>3</sub>O<sub>4</sub>@[(EtO)<sub>3</sub>Si-L<sup>1</sup>H]/Pd(0), was washed with water and dried in vacuum at 40 °C. Scheme 1 depicts the synthetic procedure for Fe<sub>3</sub>O<sub>4</sub>@[(EtO)<sub>3</sub>Si-L<sup>1</sup>H]/Pd(II). The concentration of palladium in Fe<sub>3</sub>O<sub>4</sub>@[(EtO)<sub>3</sub>Si-L<sup>1</sup>H]/Pd(0) was 4.31 wt.% as determined using ICP-AES and EDX.



**Scheme 1.** Preparation of Fe<sub>3</sub>O<sub>4</sub>@[(EtO)<sub>3</sub>Si-L<sup>1</sup>H]/Pd(II) nanocatalyst.

### Suzuki–Miyaura Coupling Reaction

In a typical reaction, 5 mg of Fe<sub>3</sub>O<sub>4</sub>@[(EtO)<sub>3</sub>Si–L<sup>1</sup>H]/Pd(II) (5 mg = 0.0021 mmol Pd) was placed in a balloon (25 mL), to which were added 1 mmol of aryl halide in 5 ml of water–ethanol (1:1), 0.134 g (1.1 mmol) of phenylboronic acid and 0.276 mg (2 mmol) of K<sub>2</sub>CO<sub>3</sub>. The mixture was then stirred for the desired time at room temperature. The reaction was monitored by TLC. After completion of the reaction, 5 ml of ethanol was added, and the catalyst was removed using an external magnet. Further purification was achieved by column chromatography.

### Heck Coupling Reaction

To a conical flask (50 ml) was added a mixture of bromobenzene (1 mmol), styrene (1.5 mmol), triethylamine (2 mmol), dimethylformamide (DMF; 3 ml) and Fe<sub>3</sub>O<sub>4</sub>@[(EtO)<sub>3</sub>Si–L<sup>1</sup>H]/Pd(II) (5 mg = 0.0021 mmol Pd) and stirred at 110 °C for 5 h (the reaction was monitored by TLC). After completion of the reaction, the reaction mixture was cooled to room temperature and the catalyst was recovered by centrifugation and washed with ethyl acetate and ethanol. The combined organic layer was dried over anhydrous sodium sulfate and evaporated in a rotary evaporator under reduced pressure. The crude product was purified by column chromatography.

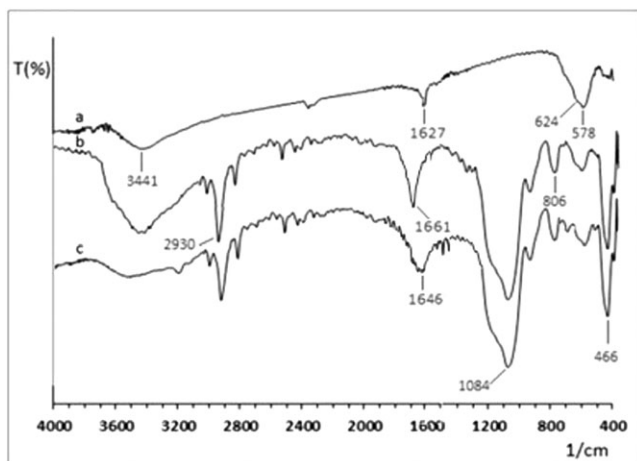
## Results and Discussion

Figure 1 shows the FT-IR absorption spectra of Fe<sub>3</sub>O<sub>4</sub> MNPs, Fe<sub>3</sub>O<sub>4</sub>@[(EtO)<sub>3</sub>Si–L<sup>1</sup>H] and Fe<sub>3</sub>O<sub>4</sub>@[(EtO)<sub>3</sub>Si–L<sup>1</sup>H]/Pd(II). The FT-IR spectrum of the unmodified Fe<sub>3</sub>O<sub>4</sub> MNPs (Fig. 1(a)) shows stretching vibrations at 3441 and 1627 cm<sup>-1</sup> which correspond to the contributions from both symmetric and asymmetric modes of the O–H bonds which are attached to the surface iron oxide NPs. The strong FT-IR absorption bands at 624 and 578 cm<sup>-1</sup> come from vibrations of Fe–O–Fe bonds of iron oxide.<sup>[33]</sup>

Comparing Figs 1(b) and (c) (spectra of Fe<sub>3</sub>O<sub>4</sub>@[(EtO)<sub>3</sub>Si–L<sup>1</sup>H] and Fe<sub>3</sub>O<sub>4</sub>@[(EtO)<sub>3</sub>Si–L<sup>1</sup>H]/Pd(II), respectively) with Fig. 1(a), the presence of the characteristic Si–O–Si peak at 1084 cm<sup>-1</sup> in Figs 1(b) and (c) is direct evidence verifying the formation of the silica shell. The peak at 2930 cm<sup>-1</sup> is attributed to the symmetric and asymmetric vibrations of methylene (–CH<sub>2</sub>–). The characteristic

organosilane and imine group vibrations (2930 and 1661 cm<sup>-1</sup>, respectively) in the FT-IR spectrum (Fig. 1(b)) of the grafted material confirm the presence of the imine group on the surface of Fe<sub>3</sub>O<sub>4</sub>. One can also see that the characteristic Fe–O–Fe peak of Fe<sub>3</sub>O<sub>4</sub> at 578 cm<sup>-1</sup> shifts to 585 cm<sup>-1</sup> in the spectrum of SiO<sub>2</sub>-coated MNPs. It is inferred that the silica shell is linked to the surface of the MNPs by a Fe–O–Si chemical bond.<sup>[34]</sup> The FT-IR spectrum of the complex (Fig. 1(c)) shows important bands from the free Schiff base ligand. The free Schiff base exhibits a broad band at 2450–2750 cm<sup>-1</sup>, attributed to hydrogen bonding between the phenolic hydrogen and azomethine nitrogen. The absence of this band in the spectrum of the covalently anchored complex indicates the loss of the hydrogen bond. The free ligand exhibits a –(C=N) stretch at 1661 cm<sup>-1</sup>; for the complex, this band shifts to lower frequency and appears at 1646 cm<sup>-1</sup> due to the coordination of the nitrogen with the Pd(II). Vibrations in the range 1480–1600 cm<sup>-1</sup> are attributed to the aromatic ring.

Figure 2 illustrates the TGA curves, depicting the variations of residual masses of the samples, obtained with a heating rate of 10 °C min<sup>-1</sup> between 30 and 800 °C. The magnetite, metal ions (palladium and silicon) and organic materials of the samples are completely converted into Fe<sub>2</sub>O<sub>3</sub> and FeO, metals and burned to generate gas products at elevated temperatures, respectively. The TGA curve of pure Fe<sub>3</sub>O<sub>4</sub> (Fig. 2(a)) shows initially a negligible weight loss (5%) in the region 90–150 °C which confirms the loss of hydrogen-bonded water molecules present at the surface of nanoferrite. A second small weight loss (2.5%) occurs in the temperature range 150–300 °C which is probably due to the removal of trapped water molecules from the lattice. Further weight loss of 3.7% is observed in the range 650–800 °C, which can be explained by decomposition of Fe<sub>3</sub>O<sub>4</sub> to FeO. Total weight loss is about 11.2%, which is due to the phase transition from Fe<sub>3</sub>O<sub>4</sub> to FeO and found to be equal to ½O<sub>2</sub>,<sup>[35]</sup> because FeO is thermodynamically stable above 570 °C in the phase diagram of the Fe–O system.<sup>[36]</sup> Figure 2(b), depicting the curve for Fe<sub>3</sub>O<sub>4</sub>@[(EtO)<sub>3</sub>Si–L<sup>1</sup>H]/Pd(II), is similar to Fig. 2(a), showing a small weight loss in the range 40–180 °C probably due to the evaporation of physically adsorbed water. A large weight loss is detected in the range 200–450 °C which is predominantly attributed to the decomposition of organic substances in Fe<sub>3</sub>O<sub>4</sub> MNPs. It is estimated that the weight loss of [(EtO)<sub>3</sub>Si–L<sup>1</sup>H] coated on the Fe<sub>3</sub>O<sub>4</sub> MNPs is about 43%.



**Figure 1.** FT-IR spectra of (a) Fe<sub>3</sub>O<sub>4</sub>, (b) Fe<sub>3</sub>O<sub>4</sub>@[(EtO)<sub>3</sub>Si–L<sup>1</sup>H] and (c) Fe<sub>3</sub>O<sub>4</sub>@[(EtO)<sub>3</sub>Si–L<sup>1</sup>H]/Pd(II).

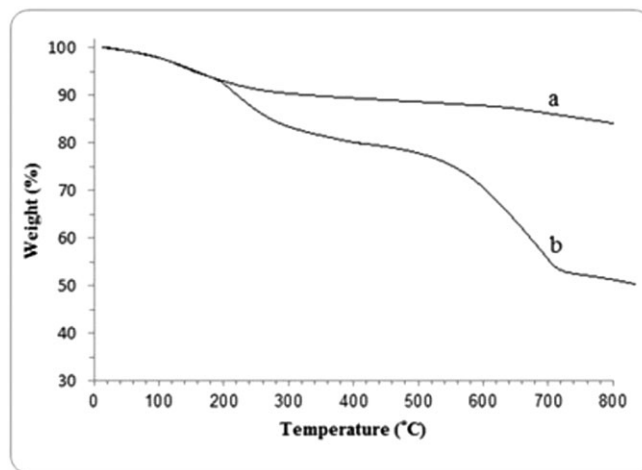


**Figure 2.** TGA curves of (a) unmodified Fe<sub>3</sub>O<sub>4</sub> MNPs and (b) Fe<sub>3</sub>O<sub>4</sub>@[(EtO)<sub>3</sub>Si–L<sup>1</sup>H]/Pd(II).

These results prove the attachment of  $[(\text{EtO})_3\text{Si-L}^1\text{H}]$  moiety onto the surface of  $\text{Fe}_3\text{O}_4$  MNPs.

The XRD patterns of  $\text{Fe}_3\text{O}_4$ ,  $\text{Fe}_3\text{O}_4@[(\text{EtO})_3\text{Si-L}^1\text{H}]$  and  $\text{Fe}_3\text{O}_4@[(\text{EtO})_3\text{Si-L}^1\text{H}]/\text{Pd(0)}$  are shown in Fig. 3. For  $\text{Fe}_3\text{O}_4$ , diffraction peaks at  $2\theta$  of  $30.4^\circ$ ,  $35.6^\circ$ ,  $43.3^\circ$ ,  $57.3^\circ$  and  $62.8^\circ$  corresponding to (220), (311), (400), (422), (511) and (440) Bragg reflections, respectively, are observed, indicative of a cubic spinel structure of the magnetite.<sup>[37]</sup> The same set of characteristic peaks is also observed for  $\text{Fe}_3\text{O}_4@[(\text{EtO})_3\text{Si-L}^1\text{H}]$  and  $\text{Fe}_3\text{O}_4@[(\text{EtO})_3\text{Si-L}^1\text{H}]/\text{Pd(0)}$ , indicating the stability of the crystalline phase of  $\text{Fe}_3\text{O}_4$  MNPs during  $[(\text{EtO})_3\text{Si-L}^1\text{H}]$  coating and Pd(0) complexation. The peak at  $2\theta = 35.6^\circ$  is chosen to calculate the average diameter using the Scherrer equation,<sup>[38]</sup> which is 17.5, 23.2 and 32.4 nm for  $\text{Fe}_3\text{O}_4$ ,  $\text{Fe}_3\text{O}_4@[(\text{EtO})_3\text{Si-L}^1\text{H}]$  and  $\text{Fe}_3\text{O}_4@[(\text{EtO})_3\text{Si-L}^1\text{H}]/\text{Pd(0)}$ , respectively. The XRD patterns of  $\text{Fe}_3\text{O}_4@[(\text{EtO})_3\text{Si-L}^1\text{H}]$  and  $\text{Fe}_3\text{O}_4@[(\text{EtO})_3\text{Si-L}^1\text{H}]/\text{Pd(0)}$  (Figs 3(b) and (c)) show an obvious diffusion peak at  $2\theta = 15\text{--}25^\circ$  that appears because of the existence of amorphous silica. The XRD pattern of  $\text{Fe}_3\text{O}_4@[(\text{EtO})_3\text{Si-L}^1\text{H}]/\text{Pd(0)}$  complex shows three major peaks at  $2\theta$  of  $39.9^\circ$ ,  $47.4^\circ$  and  $68.7^\circ$  which can be assigned to the diffraction from the four reflection indexes of (100), (200), (220) and (311), respectively (card 05-0681 in the JCPDS file).

The TEM micrographs of pure  $\text{Fe}_3\text{O}_4$  nanoparticles (Fig. 4a) and  $\text{Fe}_3\text{O}_4@[(\text{EtO})_3\text{Si-L}^1\text{H}]/\text{Pd}$  (Fig. 4b) are shown. We can see that the  $\text{Fe}_3\text{O}_4@[(\text{EtO})_3\text{Si-L}^1\text{H}]/\text{Pd}$  is nearly in core-shell structures, with black color shows  $\text{Fe}_3\text{O}_4$  and ash color is the Schiff base complex Pd shell. This indicates the successful coating on the surface of the magnetic particles. In the transmission electron microscopy images, iron oxide nanoparticles of 10-15 nm in diameter and palladium nanoparticles of  $\sim 4$  nm entrapped in iron oxide are observed.

#### Maternal Fetal Medicine

The morphologies of  $\text{Fe}_3\text{O}_4$  and  $\text{Fe}_3\text{O}_4@[(\text{EtO})_3\text{Si-L}^1\text{H}]/\text{Pd(II)}$  are clearly visible from the SEM images shown in Fig. 5. Figure 5(a) shows the SEM image of the MNPs. Figure 5(b) shows that the catalyst is made up of uniform nanometre-sized particles. It can be seen that the particles are not fully spherical. In addition, some

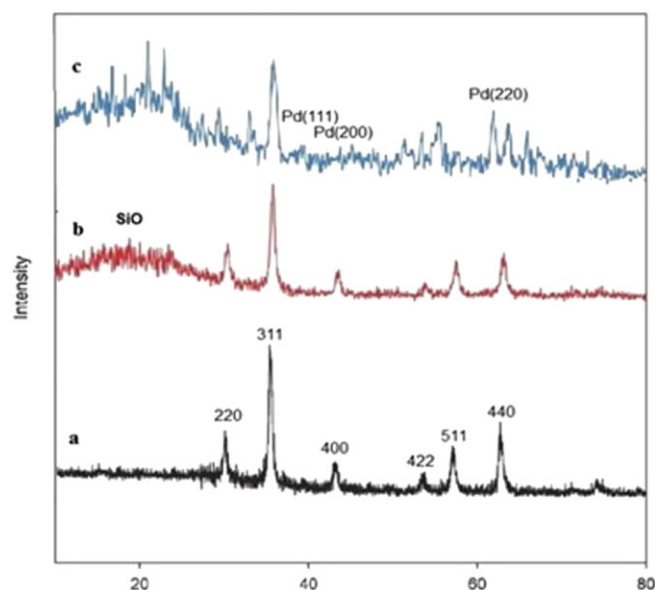


**Figure 3.** XRD patterns of (a) unmodified  $\text{Fe}_3\text{O}_4$ , (b)  $\text{Fe}_3\text{O}_4@[(\text{EtO})_3\text{Si-L}^1\text{H}]$  and (c)  $\text{Fe}_3\text{O}_4@[(\text{EtO})_3\text{Si-L}^1\text{H}]/\text{Pd(0)}$ .

particle aggregations are observed, which is likely to be caused by the magnetostatic interactions between particles.

The presence of palladium atoms in  $\text{Fe}_3\text{O}_4@[(\text{EtO})_3\text{Si-L}^1\text{H}]/\text{Pd(II)}$  is confirmed using EDX, measurements for which were recorded at random points on the surface for qualitative analysis (Fig. 6). The EDX spectrum shows the signals of iron, palladium and silicon atoms, which also indicate their presence in the composite.

The magnetic properties of  $\text{Fe}_3\text{O}_4$ ,  $\text{Fe}_3\text{O}_4@[(\text{EtO})_3\text{Si-L}^1\text{H}]$  and  $\text{Fe}_3\text{O}_4@[(\text{EtO})_3\text{Si-L}^1\text{H}]/\text{Pd(II)}$  were characterized using a vibrating sample magnetometer with an applied field of  $-8000 < H < 8000$  Oe at 300 K. These nanoparticles show high permeability in magnetization and their magnetization is sufficient for magnetic separation with an external magnetic field. Figure 7 shows the typical room temperature magnetization curves of bare  $\text{Fe}_3\text{O}_4$  MNPs,  $\text{Fe}_3\text{O}_4@[(\text{EtO})_3\text{Si-L}^1\text{H}]$  and  $\text{Fe}_3\text{O}_4@[(\text{EtO})_3\text{Si-L}^1\text{H}]/\text{Pd(II)}$ . All samples show a typical superparamagnetic behaviour. The saturation magnetization ( $M_s$ ) of  $\text{Fe}_3\text{O}_4$  MNPs at room temperature by measurement of the magnetization curve (Fig. 7) is  $54.7 \text{ emu g}^{-1}$ ; however,  $M_s$  of  $\text{Fe}_3\text{O}_4@[(\text{EtO})_3\text{Si-L}^1\text{H}]$  prepared in this study is  $52.4 \text{ emu g}^{-1}$ , which is lower than that of the bare  $\text{Fe}_3\text{O}_4$ . The reduction of measured  $M_s$  can be mainly attributed to the formation of the ligand coating on the surface of  $\text{Fe}_3\text{O}_4$  MNPs. The  $M_s$  value of  $\text{Fe}_3\text{O}_4@[(\text{EtO})_3\text{Si-L}^1\text{H}]/\text{Pd(II)}$  is markedly decreased ( $50.3 \text{ emu g}^{-1}$ )

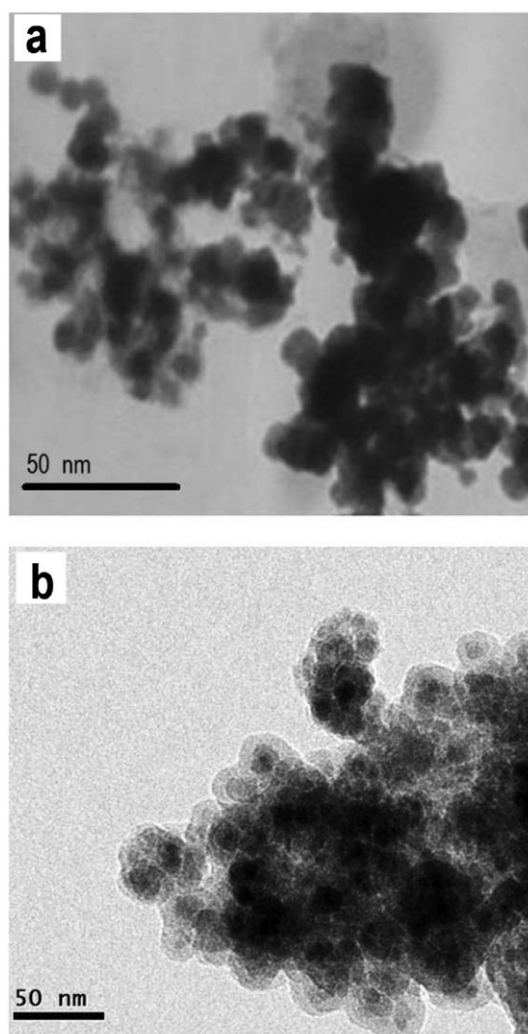


**Figure 4.** TEM images of (a)  $\text{Fe}_3\text{O}_4$  and (b)  $\text{Fe}_3\text{O}_4@[(\text{EtO})_3\text{Si-L}^1\text{H}]/\text{Pd(II)}$ .

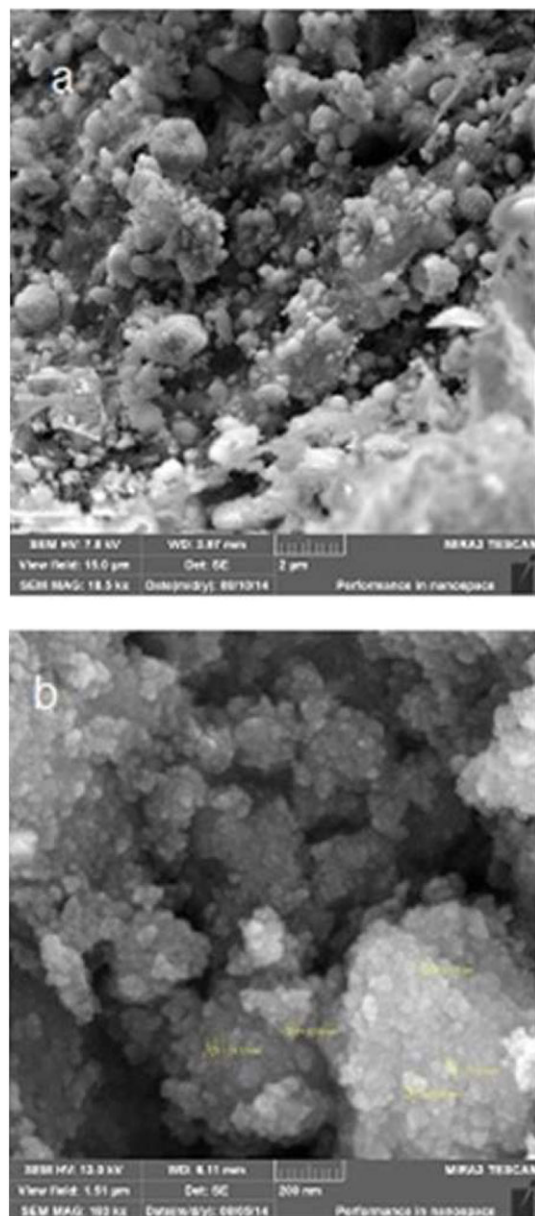


**Figure 5.** SEM images of (a) Fe<sub>3</sub>O<sub>4</sub> and (b) Fe<sub>3</sub>O<sub>4</sub>@[(EtO)<sub>3</sub>Si-L<sup>1</sup>H]/Pd(II).

due to the palladium coating and the immobilization of Fe<sub>3</sub>O<sub>4</sub>@[(EtO)<sub>3</sub>Si-L<sup>1</sup>H]. There is no hysteresis and remanent magnetization is equal to zero, suggesting that Fe<sub>3</sub>O<sub>4</sub>@[(EtO)<sub>3</sub>Si-L<sup>1</sup>H]/Pd(II) MNPs are superparamagnetic. Even with this reduction in  $M_s$ , the catalyst can still be separated from the reaction medium rapidly and easily with a magnetic field.

After structural characterization of the prepared Fe<sub>3</sub>O<sub>4</sub>@[(EtO)<sub>3</sub>Si-L<sup>1</sup>H]/Pd(II) nanocatalyst, and in continuation of our previous works,<sup>[38]</sup> its catalytic activity was investigated as an active and stable magnetically separable nanocatalyst in the Suzuki–Miyaura reaction (Scheme 2). We employed the coupling reaction of 4-bromoacetophenone with phenylboronic acid as a model reaction to study the effect of base on the reaction at room temperature and optimized the conditions.

The reaction conditions such as solvent, base and catalyst amount were optimized. Initially, the effectiveness of various solvents such as EtOH, DMF, water, EtOH–H<sub>2</sub>O and toluene was tested in the

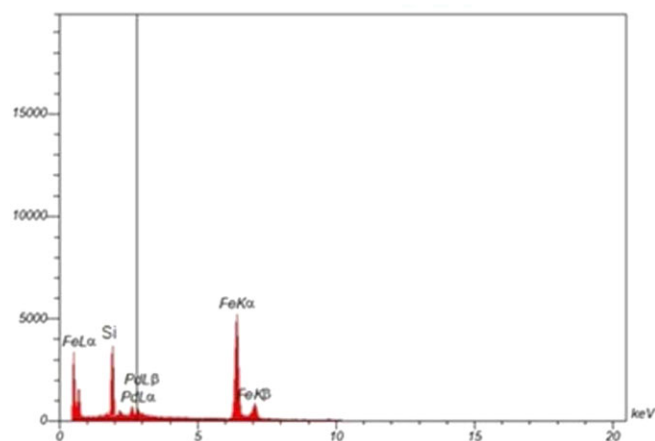


**Figure 6.** EDX analysis of the catalyst.

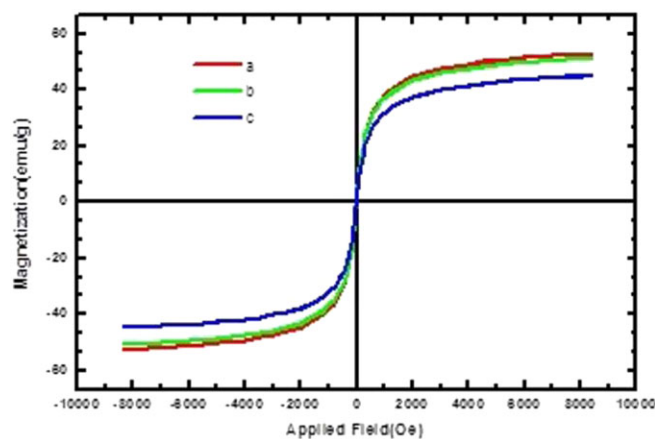
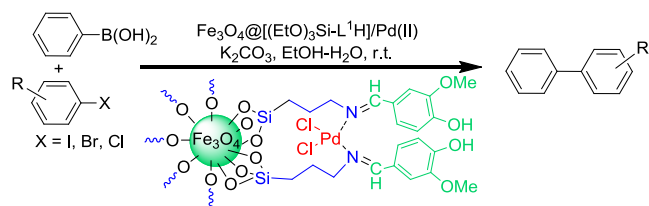


**Figure 7.** Room temperature magnetization curves of (a) Fe<sub>3</sub>O<sub>4</sub>, (b) Fe<sub>3</sub>O<sub>4</sub>@[(EtO)<sub>3</sub>Si-L<sup>1</sup>H] and (c) Fe<sub>3</sub>O<sub>4</sub>@[(EtO)<sub>3</sub>Si-L<sup>1</sup>H]/Pd(II).

Suzuki reaction. H<sub>2</sub>O–EtOH (1:1) is the best choice as solvent and this may be due to the better solubility of the reagents (Table 1). After optimizing the solvent, the reaction was run with two substrates, 4-bromoacetophenone and phenylboronic acid, in order to optimize the base. Among the bases employed (Et<sub>3</sub>N, NaOAc and K<sub>2</sub>CO<sub>3</sub>), K<sub>2</sub>CO<sub>3</sub> is found to be the most effective. The effect of catalyst loading was investigated employing different quantities of the catalyst ranging from 0.1 to 0.3 mol% (Table 1, entries 5, 8 and 9). The best result is obtained with 0.005 g (0.2 mol%) of the catalyst.

Using the optimized reaction conditions, the catalyst was applied to a representative phenylboronic acid with a range of aryl halides (I, Br, Cl). The results are summarized in Table 2. For the activated electron-deficient substrate, aryl couples with phenylboronic acid to give a relatively high yield of product (Table 2, entry 12). Various electron-donating and electron-withdrawing groups such as –CH<sub>3</sub>, –OCH<sub>3</sub>, –NO<sub>2</sub>, –COCH<sub>3</sub> and –CHO on both aryl bromide and iodide are well tolerated affording the desired unsymmetric biaryls in good to excellent yields. Under those conditions, iodobenzene, *p*-iodotoluene and *p*-iodoanisole react very cleanly with phenylboronic acid in good yields (Table 2, entries 1, 4 and 12). It is found that the yield when using an *ortho*-substituted aryl bromide is lower (Table 2, entry 7) than those when using *para*- or *meta*-substituted aryl bromides (Table 2, entries 5, 9, 11, 13 and 14).



**Scheme 2.**  $\text{Fe}_3\text{O}_4@[[(\text{EtO})_3\text{Si-L}^1\text{Hj}]/\text{Pd(II)}]$  catalysing Suzuki cross-coupling reaction.

**Table 1.** Optimization of conditions for Suzuki–Miyaura reaction of 4-bromoacetophenone with phenylboronic acid<sup>a</sup>

Entry	Solvent	Pd (mol%)	Base	Time (min)	Yield (%) <sup>b</sup>
1	DMF	0.2	$\text{K}_2\text{CO}_3$	80	80
2	Toluene	0.2	$\text{K}_2\text{CO}_3$	60	65
3	EtOH	0.2	$\text{K}_2\text{CO}_3$	60	77
4	$\text{H}_2\text{O}$	0.2	$\text{K}_2\text{CO}_3$	90	55
5	$\text{EtOH-H}_2\text{O}^c$	0.2	$\text{K}_2\text{CO}_3$	40	99
6	$\text{EtOH-H}_2\text{O}^c$	0.2	NaOAc	60	65
7	$\text{EtOH-H}_2\text{O}^c$	0.2	$\text{Et}_3\text{N}$	90	80
8	$\text{EtOH-H}_2\text{O}^c$	0.1	$\text{K}_2\text{CO}_3$	60	75
9	$\text{EtOH-H}_2\text{O}^c$	0.3	$\text{K}_2\text{CO}_3$	60	96
10	$\text{EtOH-H}_2\text{O}^c$	0.2	No base	90	Trace

<sup>a</sup>Reaction conditions: 4-bromoacetophenone (1 mmol),  $\text{PhB(OH)}_2$  (1.1 mmol),  $\text{Fe}_3\text{O}_4@[[(\text{EtO})_3\text{Si-L}^1\text{Hj}]/\text{Pd(II)}]$ , solvent (3 ml).

<sup>b</sup>Isolated yield.

<sup>c</sup> $\text{EtOH-H}_2\text{O} = 1:1$ .

**Table 2.** Heterogeneous Suzuki–Miyaura reaction of aryl halides with phenylboronic acid catalysed by  $\text{Fe}_3\text{O}_4@[[(\text{EtO})_3\text{Si-L}^1\text{Hj}]/\text{Pd(II)}]$  at room temperature<sup>a</sup>

Entry	R	X	Time (h)	Yield (%) <sup>b</sup>
1	H	I	0.20	99
2	H	Br	0.50	98
3	H	Cl	6.00	86
4	4- $\text{CH}_3\text{O}$	I	0.40	98
5	4- $\text{CH}_3\text{O}$	Br	1.25	98
6	2- $\text{CH}_3\text{O}$	I	0.50	93
7	2- $\text{CH}_3\text{O}$	Br	1.50	91
8	4- $\text{NO}_2$	I	1.25	96
9	4- $\text{NO}_2$	Br	2.15	91
10	4-CHO	I	3.10	92
11	4-CHO	Br	4.50	77
12	4- $\text{CH}_3$	I	0.30	99
13	4- $\text{CH}_3$	Br	1.10	95
14	4- $\text{COCH}_3$	Br	0.66	98
15	2- $\text{NO}_2$	I	3.05	90
16	2- $\text{NO}_2$	Br	4.10	88

<sup>a</sup>Reactions were carried out under aerobic conditions in 3 ml of  $\text{H}_2\text{O-EtOH}$  (1:1), with 1.0 mmol of aryl halide, 1.1 mmol of phenylboronic acid and 2 mmol of  $\text{K}_2\text{CO}_3$  in the presence of catalyst (0.005 g, 0.2 mol % Pd).

<sup>b</sup>Isolated yield.

The results show that  $\text{Fe}_3\text{O}_4@[[(\text{EtO})_3\text{Si-L}^1\text{Hj}]/\text{Pd(II)}]$  is a good catalyst for the Suzuki cross-coupling reaction by giving good yield with high purity for aryl bromides and aryl iodides (Table 2, entries 1, 2, 4–14). However, this catalyst gives poor yield with aryl chlorides under the same reaction condition (Table 2, entry 3).

After the completion of the reaction, the catalyst can be recovered by simple filtration and washed with solvents to remove all the impurities. Therefore, the Pd complex is a good heterogeneous catalyst for Suzuki cross-coupling reaction. A filtration test was carried out to investigate the amounts of active Pd species that leach out into the solution during the reaction. Each supported Pd catalyst was placed under the Suzuki reaction conditions and supernatant collected. The filtrate was then used for a Suzuki cross-coupling reaction between 4-bromoacetophenone and boronic acid. The filtrate from  $\text{Fe}_3\text{O}_4@[[(\text{EtO})_3\text{Si-L}^1\text{Hj}]/\text{Pd(II)}]$  afforded conversions of 1%, indicating that a minimal amount of Pd leached out from the catalyst. These studies demonstrate that only the Pd bound to  $\text{Fe}_3\text{O}_4@[[(\text{EtO})_3\text{Si-L}^1\text{Hj}]]$  during the reaction is active, and the reaction proceeds on the heterogeneous surface.

In order to investigate the recyclability of the Pd catalyst, the Suzuki cross-coupling reaction between phenylboronic acid and 4-bromoacetophenone was examined (Fig. 8). The catalyst shows consistent catalytic activity during five runs. The results show that the Pd catalyst can be reused at least five times with no significant loss of catalytic activity, with simple filtration and washing. In order to regenerate the catalyst, after each cycle, it was separated using a magnet, and washed several times with deionized water and ethanol. Then, it was dried in oven at  $50^\circ\text{C}$  and used in the next run. The leaching of Pd into the reaction mixture from the recovered supported complex was analysed using ICP-MS. The results show that this catalyst can be reused five times without any significant loss in activity performance (Fig. 8).

In order to evaluate catalytic activity of the prepared  $\text{Fe}_3\text{O}_4@[[(\text{EtO})_3\text{Si-L}^1\text{Hj}]/\text{Pd(II)}]$  hybrid material as a heterogeneous nanocatalyst, the Heck coupling reaction between bromobenzene and styrene as a model reaction was investigated (Scheme 3). The best result (96% yield) is obtained with 1 mol% catalyst in the presence of  $\text{Et}_3\text{N}$  as base in DMF. After optimizing the reaction

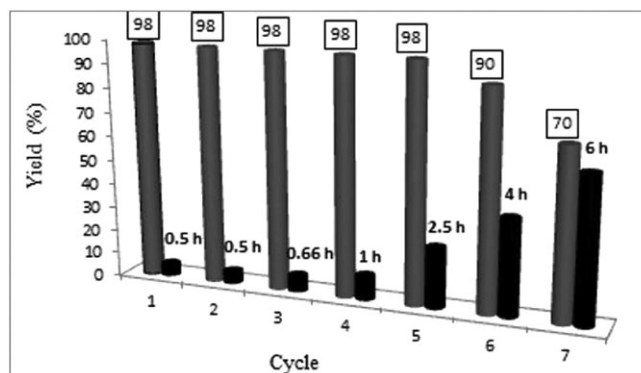
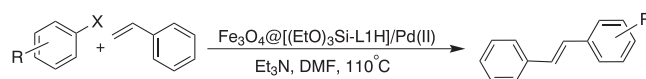


**Figure 8.** Recycling of  $\text{Fe}_3\text{O}_4@[[(\text{EtO})_3\text{Si-L}^1\text{Hj}]/\text{Pd(II)}]$  for the Suzuki coupling reaction under similar conditions.



**Scheme 3.**  $\text{Fe}_3\text{O}_4@[[(\text{EtO})_3\text{Si-L}^1\text{Hj}]/\text{Pd(II)}]$  catalysing Heck coupling reaction.

**Table 3.** Heck reaction of aryl halides and styrene catalysed by Fe<sub>3</sub>O<sub>4</sub>@[(EtO)<sub>3</sub>Si-L<sup>1</sup>H]/Pd(II)<sup>a</sup>

Entry	R	X	Time (h)	Yield (%) <sup>b</sup>	M.p. (°C)	
					Found	Reported
1	H	I	2	98	122–124	121–123 <sup>[39]</sup>
2	H	Br	3	96	122–124	121–123 <sup>[39]</sup>
3	4-CH <sub>3</sub> O	I	5	96	134–136	135–137 <sup>[39]</sup>
4	4-CH <sub>3</sub> O	Br	7	92	134–136	135–137 <sup>[39]</sup>
5	4-CH <sub>3</sub>	I	4	95	118–120	117–119 <sup>[40]</sup>
6	4-CH <sub>3</sub>	Br	5	90	118–120	117–119 <sup>[40]</sup>

<sup>a</sup>Reaction conditions: aryl halide (1 mmol), styrene (1.5 mmol), Fe<sub>3</sub>O<sub>4</sub>@[(EtO)<sub>3</sub>Si-L<sup>1</sup>H]/Pd(II) (5 mg = 0.0021 mmol Pd), Et<sub>3</sub>N (2 mmol), DMF (3 ml).<sup>b</sup>Isolated yield.

conditions according to our previous report,<sup>[38]</sup> the scope and generality of the developed protocol with respect to aryl bromide and aryl iodide structure were investigated by using 1 mol% of Fe<sub>3</sub>O<sub>4</sub>@[(EtO)<sub>3</sub>Si-L<sup>1</sup>H]/Pd(II) in the presence of 2 equiv. of Et<sub>3</sub>N in DMF at 110 °C. The results are summarized in Table 3.

## Conclusions

We have successfully prepared Fe<sub>3</sub>O<sub>4</sub> MNPs and coated them with [(EtO)<sub>3</sub>Si-L<sup>1</sup>H] as organic shell via a co-precipitation method. A Pd(II) Schiff base complex has been immobilized on the MNPs through a surface modification of Fe<sub>3</sub>O<sub>4</sub> with a Schiff base ligand. The catalyst was found to be easily reusable several times after recovery by separation and drying without significant catalytic deactivation which typically happens due to the leaching of active species or degradation of the structure. The Pd complex is a good heterogeneous catalyst for Suzuki cross-coupling reaction of various aryl halides (I, Br, Cl) with phenylboronic acid and Heck coupling reaction between aryl halides (I, Br) and styrene.

## Acknowledgements

We are grateful to the Bu-Ali Sina University and Payame Noor University for their partial support of this project.

## References

- [1] A. J. Suzuki, *Organometal. Chem.* **1999**, 576, 147.
- [2] J. P. Tremblay-Morin, H. Ali, J. E. van Lier, *Tetrahedron Lett.* **2006**, 47, 3043.
- [3] S. Lightowler, M. Hird, *Chem. Mater.* **2005**, 17, 5538.
- [4] X. Zhan, S. Wang, Y. Liu, X. Wu, D. Zhu, *Chem. Mater.* **2003**, 15, 1963.
- [5] S. D. Walker, T. E. Barder, J. R. Martinelli, S. L. Buchwald, *Angew. Chem. Int. Ed.* **2004**, 43, 1871.
- [6] H. Zhang, Q. Zhu, Y. Zhang, Y. Wang, L. Zhao, B. Yu, *Adv. Funct. Mater.* **2007**, 17, 2766.
- [7] A. Hu, G. T. Yee, W. Lin, *J. Am. Chem. Soc.* **2005**, 127, 12486.
- [8] K. K. Senapati, C. B. Orgohain, P. Phukan, *J. Mol. Catal. A* **2011**, 33, 924.
- [9] C. W. Lim, I. S. Lee, *Nano Today* **2010**, 5, 412.
- [10] H. Gu, R. Zheng, X. Zhang, B. Xu, *J. Am. Chem. Soc.* **2004**, 126, 5664.
- [11] J. Gao, B. Zhang, Y. Gao, Y. Pan, X. Zhang, B. Xu, *J. Am. Chem. Soc.* **2007**, 129, 11928.
- [12] T. J. Yoon, K. N. Yu, E. Kim, J. S. Kim, B. G. Kim, S. H. Yun, B. H. Sohn, M. H. Cho, J. K. Lee, S. B. Park, *Small* **2006**, 2, 209.
- [13] S. Y. Yu, H. J. Zhang, J. B. Yu, C. Wang, L. N. Sun, W. D. Shi, *Langmuir* **2007**, 23, 7836.
- [14] X. Yu, J. Wan, Y. Shan, K. Chen, X. Han, *Chem. Mater.* **2009**, 21, 4892.
- [15] R. Ghorbani-Vaghei, S. Hemmati, H. Veisi, *J. Mol. Catal. A* **2014**, 393, 240.
- [16] K. C. Nicolaou, C. N. C. Boddy, S. Brase, N. Winssinger, *Angew. Chem. Int. Ed.* **1999**, 38, 2096.
- [17] N. E. Leadbeater, *Chem. Commun.* **2005**, 2881.
- [18] S. Mohanty, D. Suresh, M. S. Balakrishna, J. T. Mague, *Tetrahedron* **2008**, 64, 240.
- [19] N. Miyaura, T. Yanagi, A. Suzuki, *Synth. Commun.* **1981**, 11, 513.
- [20] J. P. Wolfe, R. A. Singer, B. H. Yang, S. L. Buchwald, *J. Am. Chem. Soc.* **1999**, 121, 9550.
- [21] A. N. Cammidge, N. J. Baines, R. K. Bellingham, *Chem. Commun.* **2001**, 2588.
- [22] L. Canali, D. C. Sherrington, *Chem. Soc. Rev.* **1999**, 28, 85.
- [23] T. Katsuki, *Coord. Chem. Rev.* **1995**, 140, 189.
- [24] R. Skoda-Földes, L. Kollár, A. Arcadi, *J. Mol. Catal.* **1995**, 101, 37.
- [25] B. S. Lane, K. Burgess, *Chem. Rev.* **2003**, 103, 2457.
- [26] G. Righi, C. Bonini, *Synthesis* **1994**, 3, 225.
- [27] G. X. Zheng, J. J. Eisch, Z. R. Lui, X. Ma, *J. Org. Chem.* **1992**, 57, 5140.
- [28] L. P. C. Nielson, C. P. Stevenson, D. G. Backmond, E. N. Jacobsen, *J. Am. Chem. Soc.* **2004**, 126, 1360.
- [29] J. Lopez, S. Liang, X. R. Bu, *Tetrahedron Lett.* **1998**, 39, 4199.
- [30] A. M. Daly, C. T. Dalton, M. F. Renehan, D. G. Gilheany, *Tetrahedron Lett.* **1999**, 40, 3617.
- [31] R. Y. Hong, T. T. Pana, H. Z. Li, *J. Magn. Magn. Mater.* **2006**, 30, 360.
- [32] I. C. Chisem, J. Rafelt, M. T. Shieh, J. Chisem, J. H. Clark, R. Jachuck, D. Macquarrie, C. Ramshav, K. Scott, *Chem. Commun.* **1949**, 1998.
- [33] Z. M. Rao, T. H. Wu, S. Y. Peng, *Acta Phys. -Chim. Sin.* **1995**, 11, 395.
- [34] F. H. Chen, Q. Gao, J. Z. Ni, *Nanotechnology* **2008**, 19, 165103.
- [35] S. Y. Zhao, D. K. Lee, C. W. Kim, H. G. Cha, Y. H. Kim, Y. S. Kang, *Bull. Kor. Chem. Soc.* **2006**, 27, 237.
- [36] L. S. Darken, R. W. Gurry, *J. Am. Chem. Soc.* **1946**, 68, 798.
- [37] T. Z. Yang, C. M. Shen, H. J. Gao, *J. Phys. Chem. B* **2005**, 9, 23233.
- [38] (a) H. Keypour, M. Balalia, M. M. Haghdooost, M. Bagherzadeh, *RSC Adv.* **2012**, 00, 1. (b) M. Aghayee, M. A. Zolfilog, H. Keypour, M. Yarie, L. Mohammadi, *Appl. Organomet. Chem.* **2016**, 30, 612. (c) H. Veisi, R. Masti, D. Kordestani, M. Safaei, O. Sahin, *J. Mol. Catal. A: Chem.* **2014**, 384, 61. (d) H. Veisi, A. Sedrpoushan, B. Maleki, M. Hekmati, M. Heidari, S. Hemmati, *Appl. Organomet. Chem.* **2015**, 29, 834. (e) H. Veisi, A. Sedrpoushan, S. Hemmati, *Appl. Organomet. Chem.* **2015**, 29, 825. (f) M. Pirhayati, H. Veisi, A. Kakanejadifard, *RSC Adv.* **2016**, 6, 27252. (g) H. Veisi, N. Morakabati, *New J. Chem.* **2015**, 39, 2901. (h) H. Veisi, D. Kordestani, A. R. Faraji, *J. Porous Mater.* **2014**, 21, 141.
- [39] N. Iranpoor, H. Firouzabadi, A. Tarassoli, M. Fereidoonnazhad, *Tetrahedron* **2010**, 66, 2415.
- [40] R. J. Kalbasi, N. Mosaddegh, A. Abbaspourrad, *Tetrahedron Lett.* **2012**, 53, 3763.